Supplement of Atmos. Chem. Phys., 21, 14199–14213, 2021
https://doi.org/10.5194/acp-21-14199-2021-supplement

Atmospheric Chemistry and Physics
Open Access

Supplement of

Measurement report: The chemical composition of and temporal variability in aerosol particles at Tuktoyaktuk, Canada, during the Year of Polar Prediction Second Special Observing Period

John MacInnis et al.

Correspondence to: Rachel Ying-Wen Chang (rachel.chang@dal.ca)

Table S1. Masses and detection frequencies of ions and metals in fine ($PM_{2.5}$) and coarse ($PM_{10-2.5}$) aerosol filter samples from Tuktoyaktuk. Means were calculated using masses equal to or greater than the detection limit (DL).

	Particle Size	DL (µg)	Mean (µg)	Range (µg)	Frequency (%)
Ions					
F^-	$PM_{2.5}$	2.4	<2.4	<2.4	0
	$PM_{10–2.5}$		2.5	<2.4-2.7	25
Cl^-	$PM_{2.5}$	0.020	0.45	<0.020-1.2	62
	$PM_{10–2.5}$		<0.020	<0.020	0
NO_2^-	$PM_{2.5}$	0.050	<0.050	<0.050	0
	$PM_{10–2.5}$		0.10	<0.050-0.10	12
Br^-	$PM_{2.5}$	0.090	<0.090	<0.090	0
	$PM_{10–2.5}$		0.19	<0.090-0.19	25
NO_3^-	$PM_{2.5}$	0.39	0.40	<0.39-0.40	25
	$PM_{10–2.5}$		0.42	<0.39-0.42	12
PO_4^{3-}	$PM_{2.5}$	0.12	0.61	<0.12-0.87	25
	$PM_{10–2.5}$		1.1	<0.12-1.4	37
SO_4^{2-}	$PM_{2.5}$	0.17	0.48	<0.17-1.2	87
	$PM_{10–2.5}$		<0.17	<0.17	0
NH_4^+	$PM_{2.5}$	0.19	0.21	<0.19-0.21	12
	$PM_{10–2.5}$		<0.19	<0.19	0
Ca^{2+}	$PM_{2.5}$	0.28	0.72	<0.28-0.95	25
	$PM_{10–2.5}$		<0.28	<0.28	0
Metals					
Al	$PM_{2.5}$	0.030	0.089	0.030-0.3	100
	$PM_{10–2.5}$		0.054	<0.030-0.078	75
Fe	$PM_{2.5}$	0.13	0.26	<0.13-0.26	25
	$PM_{10–2.5}$		0.16	<0.13-0.16	12
Ag	$PM_{2.5}$	0.0024	<0.0024	<0.0024	0
	$PM_{10–2.5}$		0.0026	<0.0024-0.0029	25
Ti	$PM_{2.5}$	0.0030	0.0052	<0.0030-0.0074	25
	$PM_{10–2.5}$		<0.0030	<0.0030	0
Cu	$PM_{2.5}$	0.012	<0.012	<0.012	0
	$PM_{10–2.5}$		0.013	<0.012-0.013	12
Sb	$PM_{2.5}$	0.012	0.029	<0.012-0.029	12
	$PM_{10–2.5}$		0.021	<0.012-0.021	12
Ba	$PM_{2.5}$	0.019	<0.019	<0.019	0
	$PM_{10–2.5}$		0.047	<0.019-0.072	37
Zn	$PM_{2.5}$	0.0080	0.011	<0.0080-0.011	25
	$PM_{10–2.5}$		0.011	<0.0080-0.012	37

Table S2. An overview of formulas used for mass reconstruction analysis, adapted from Bari and Kindzierski, 2017. The chemical masses of ions and metals were used in formulas.

Component	Formula
$(NH_4)_2SO_4$	$[(NH_4)_2SO_4] = [SO_4^{2-}] + [NH_4^+] – 0.29[NO_3^-]$
NH_4NO_3	$[NH_4NO_3] = 1.29[NO_3]$
NaCl	$[NaCl] = 1.65[Cl^-]$
Mineral Dust (MD)	$[MD] = 2.20[Al] + 1.63[Ca^{2+}] + 2.42[Fe] + 1.94[Ti]$
Metal Oxides (MO)	$[MO] = 1.25[Cu] + 1.24[Zn] + 1.07[Ag] + 1.20[Sb] + 1.12[Ba]$
Particle-bound water (PBW)	$[PBW] = 0.32[SO_4^{2-} + NH_4^+]$
Unclassified Inorganic (UI)	$[UI] = [F^-] + [Br^-] + [PO_4^{3-}] + [NO_2^-]$

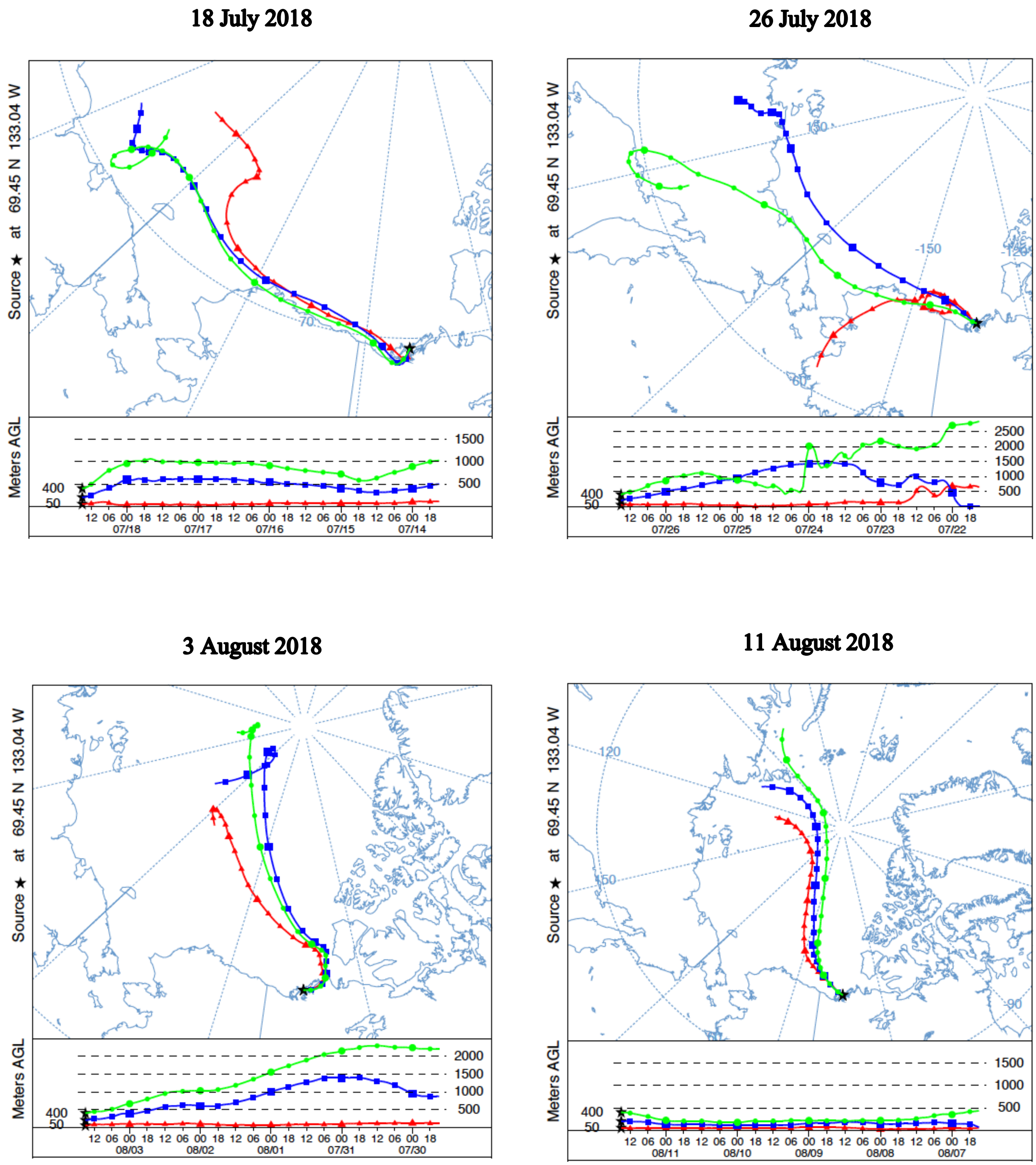

Figure S1. Air mass back trajectories (120 h) during 18 July to 11 August using the HYSPLIT Model (National Oceanic and Atmospheric Administration, https://www.ready.noaa.gov/HYSPLIT_traj.php) with Global Data Assimilation System meteorology at heights of 50, 200, and 400 m above ground level.

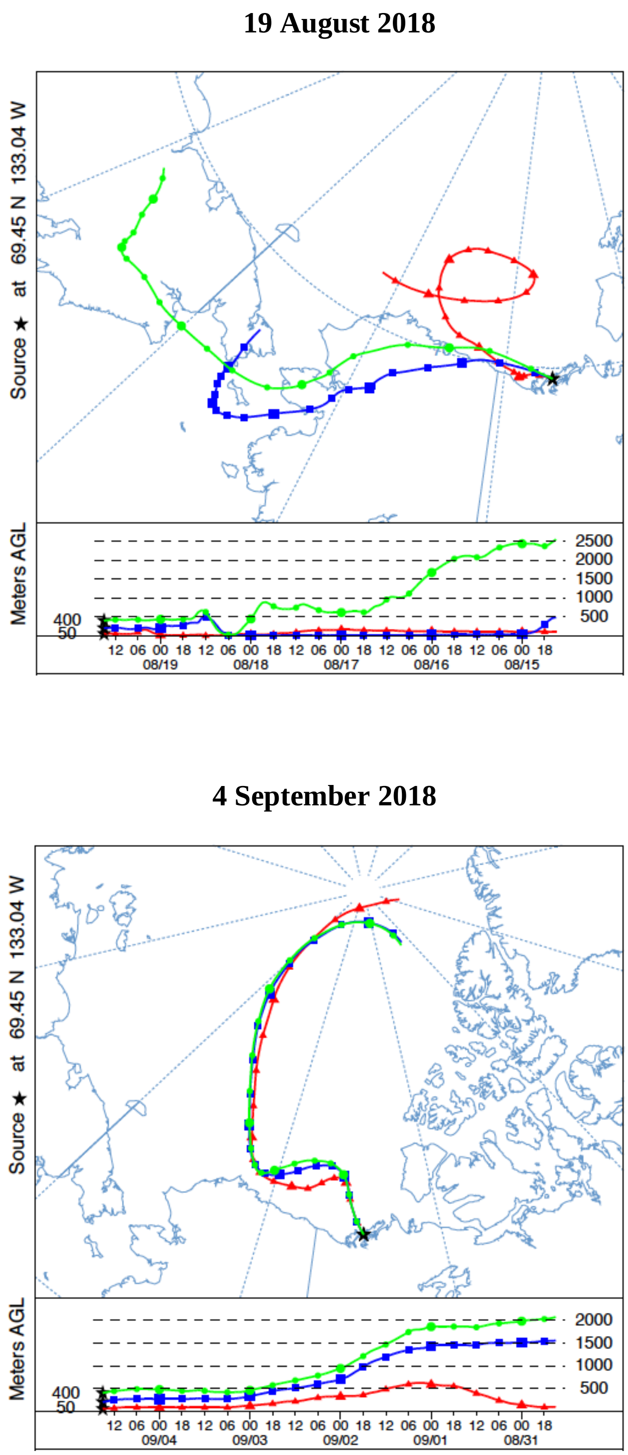

Figure S2. Air mass back trajectories (120 h) during 19 August to 12 September using the HYSPLIT Model (National Oceanic and Atmospheric Administration, https://www.ready.noaa.gov/HYSPLIT_traj.php) with Global Data Assimilation System meteorology at heights of 50, 200, and 400 m above ground level.

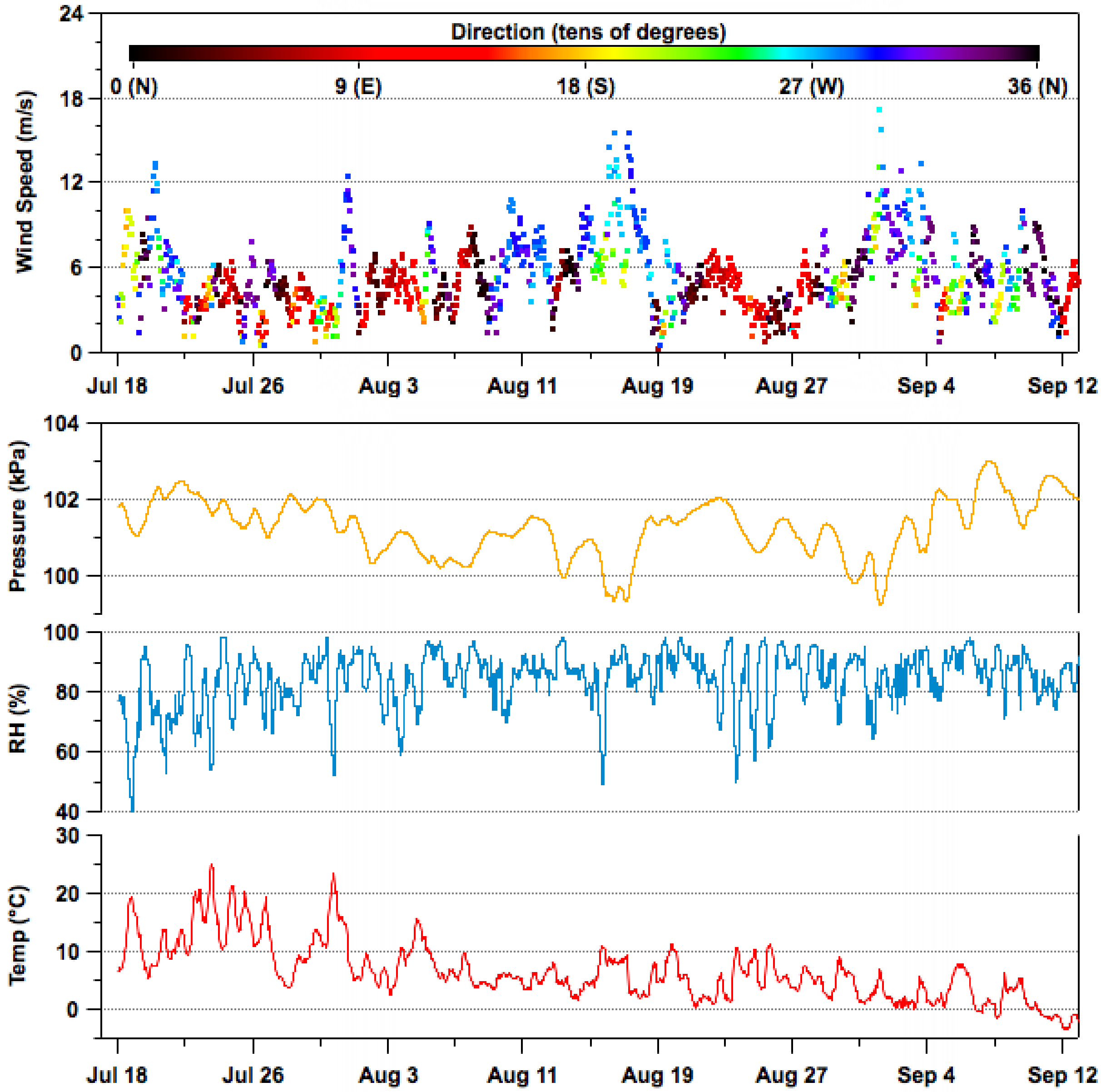

Figure S3. Hourly wind speed and direction, atmospheric pressure, relative humidity (RH), and temperature data recorded at the Tuktoyaktuk airport from 18 July to 12 September 2018. A wind direction of 36 corresponds to wind originating from the geographic north pole, while a wind direction of 9 corresponds to a wind originating from the east. The data presented in this figure can be found in Historical Climate Archives (Environment and Climate Change Canada 2020).

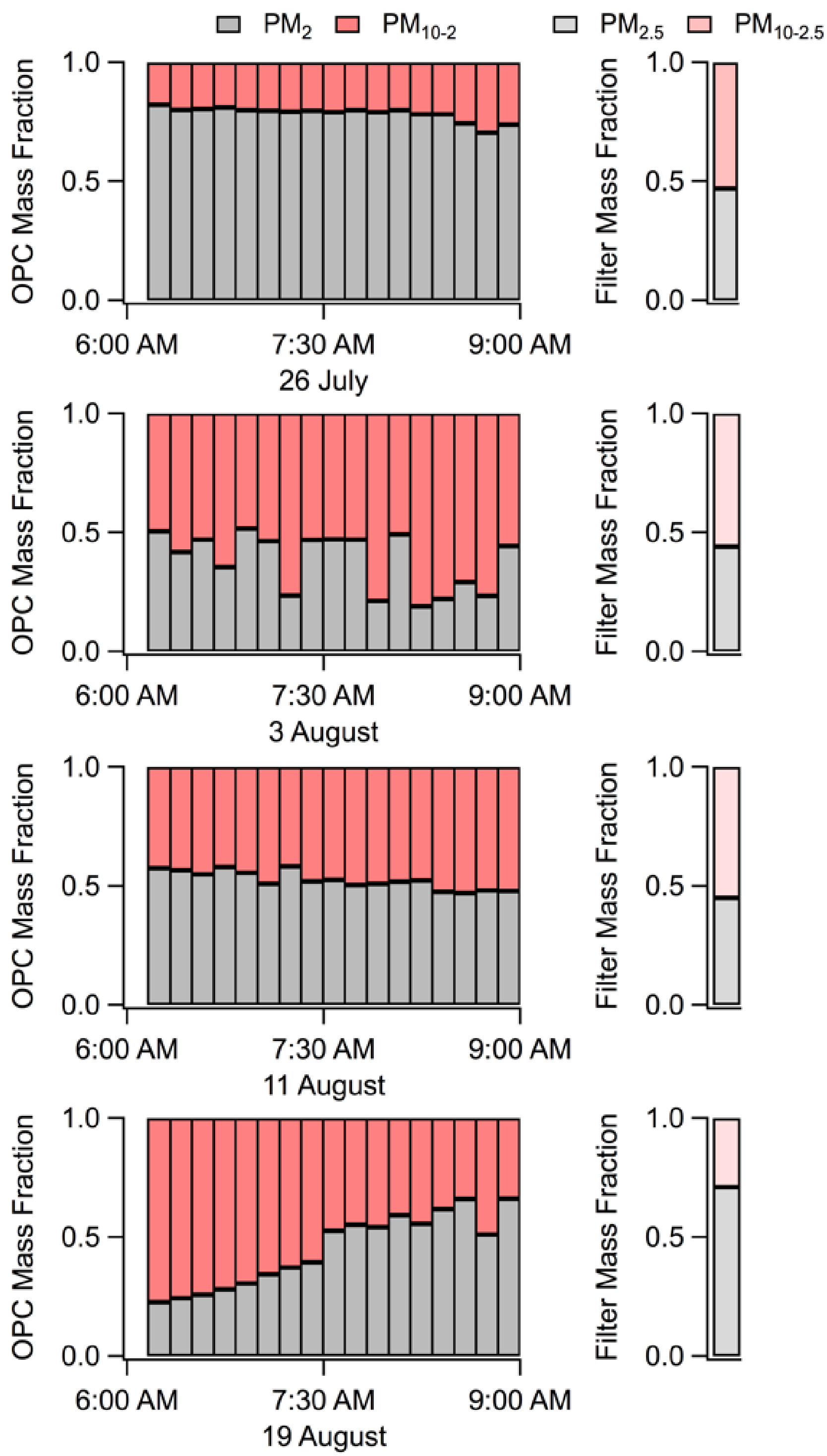

Figure S4. Comparison of mass fractions between the optical particle counter (OPC) and filter analyses during 26 July and 3, 11, and 19 August 2018. For the OPC analysis, PM_2 corresponds to aerosol particles in 0.3-0.5, 0.5-1, and 1-2 μm bins, while PM_{10-2} corresponds to aerosol particles in 2-5 and 5-10 μm bins. These dates were selected for comparison because there are available instrument log files confirming the sampling duration (6:00 to 9:00 AM local time).

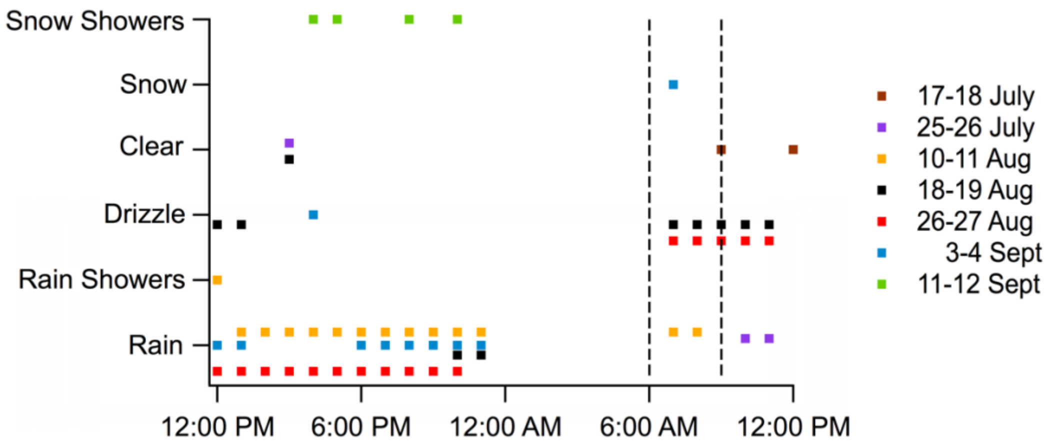

Figure S5. Hourly weather condition time series recorded at the Tuktoyaktuk airport from 17 July to 12 September 2018. Dashed vertical lines demarcate the estimated sampling times for aerosol filter samples, corresponding to 6:00 to 9:00 AM local time. Note that cloudy conditions were only observed on 3 August, which is not included in this figure, and no observations were recorded from 12:00 to 6:00 AM local time. The data presented in this figure can be found in Historical Climate Archives (Environment and Climate Change Canada 2020).

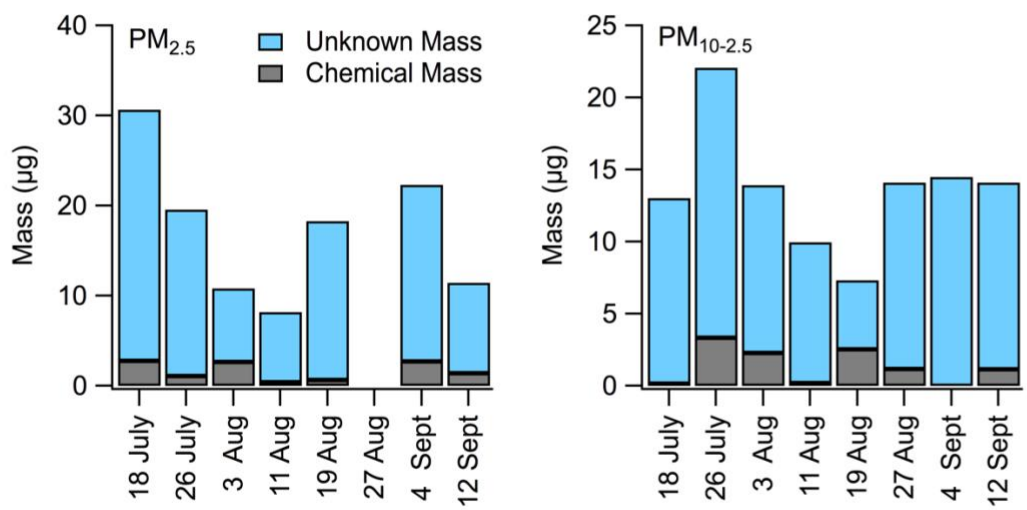

Figure S6. Overview of the chemical and unknown mass in fine ($PM_{2.5}$) and coarse ($PM_{10-2.5}$) aerosol filter samples from Tuktoyaktuk from 18 July to 12 September. The chemical mass in filters was calculated according to equations in Table S2, and the unknown mass is calculated as the difference between the total gravimetric mass and the chemical mass. Note that 27 August in $PM_{2.5}$ is not included in this analysis, as the chemical mass was greater than the gravimetric mass.

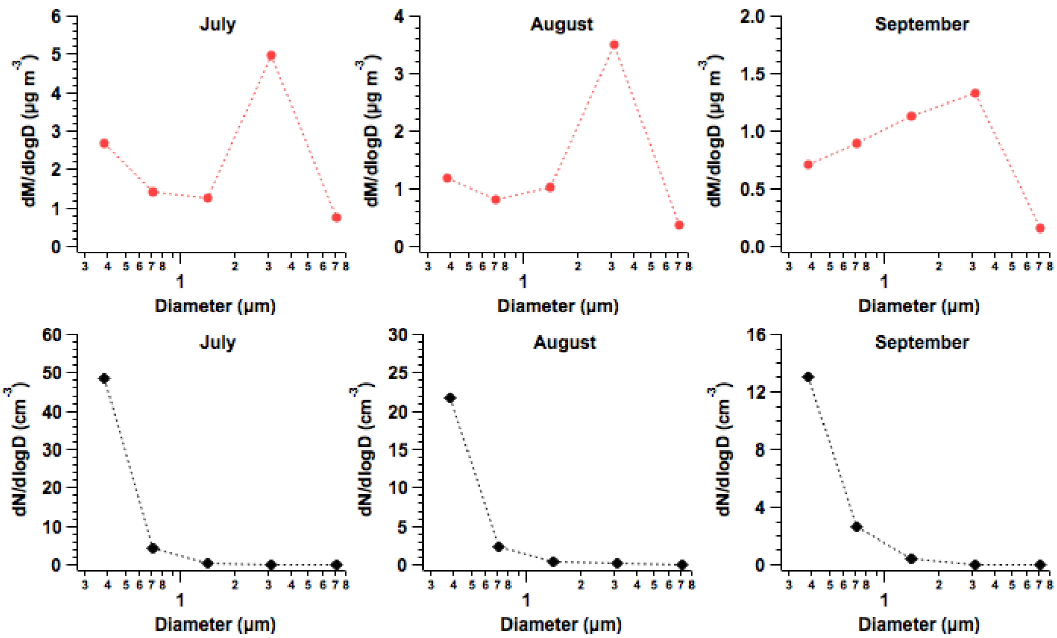

Figure S7. Average number (bottom row) and mass (top row) size distributions of aerosol particles collected from Tuktoyaktuk during July-September 2018. The x-axis refers to the geometric mean bin diameters for the optical particle counter.

References

Bari, M.A., and Kindzierski, W.B.:Ambient fine particulate matter ($PM_{2.5}$) in Canadian oil sands communities: Levels, sources and potential human health risk. Sci. Total Environ. **595**: 828–838. doi:10.1016/j.scitotenv.2017.04.023., 2017.

Environment and Climate Change Canada. 2020. Historical Climate Data: https://climate.weather.gc.ca/historical_data/search_historic_data_stations_e.html?searchType=stnName&timeframe=1&txtStationName=tuktoyaktuk&searchMethod=contains&optLimit=yearRange&StartYear=1840&EndYear=2020&Year=2020&Month=9&Day=7&selRowPerPage=25, last access: 15 September 2020.